Selected Paper

Thermal Isomerization at a C=N Double Bond: How Does the Mechanism Vary with the Substituent?

Hiroshi Yamataka,* Salai Cheettu Ammal, Tsutomu Asano,[1] and Yasushi Ohga[1]

Department of Chemistry, Rikkyo University, Nishi-Ikebukuro, Toshima-ku, Tokyo 171-8501

[1]Department of Applied Chemistry, Faculty of Engineering, Oita University, 700 Dannoharu, Oita 870-1192

Received May 18, 2005; E-mail: yamataka@rikkyo.ac.jp

Thermal isomerizations at the C=N double bonds in $R_1R_2C{=}NC_6H_4X$ proceed via an inversion mechanism, in which the $C{=}NC_6H_4X$ bond angle is near 180° at the transition state (TS). Available experimental data on the reactions of $(CF_3)_2C{=}NC_6H_4X$ and $YC_6H_4CH{=}NC_6H_4X$ have suggested that the reaction mechanism changes with substituent X. In the present study, HF, B3LYP, and MP2 computations were carried out to analyze the modes of mechanistic change with the substituent for the reactions of $(CF_3)_2C{=}NC_6H_4X$, $YC_6H_4CH{=}NC_6H_4X$, and other systems. There are two possible pathways within the inversion mechanistic framework: a planar pathway with the $R_1R_2C{=}N$ double-bond plane and the aromatic ring being coplanar at the TS and a perpendicular one with the two planes being perpendicular to each other at the TS. It was found that the mechanistic change is not due to a change in the relative importance of two independent and competitive reaction pathways, but arises from a change of the character of a single TS from planar to perpendicular geometry when the substituent becomes more electron-withdrawing.

Thermal isomerization at the C=N bond of imine derivatives of aniline is an intriguing reaction, in which the reaction mechanism readily changes with the structure of the reactant (Eq. 1).[1–10] Three mechanisms are conceivable for isomerization of the double bond in general: rotation, inversion-perpendicular, and inversion-planar mechanisms. In the rotation mechanism, a rotation of the C=N double bond is the main reaction coordinate with little change of the bond angle (θ) in Eq. 1. The reaction coordinate in the inversion mechanisms is a change in the angle θ, and at the transition state (TS), θ becomes nearly 180°. The torsional angle (ϕ) at the TS is close to 90° in the inversion-perpendicular mechanism, whereas it is nearly 0° in the inversion-planar mechanism.

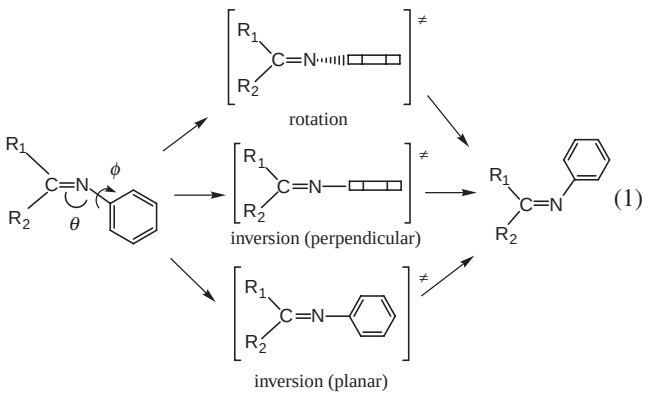

(1)

Roberts et al. reported in 1971 that the reaction of the C=N isomerization of *N*-[2,2,2-trifluoro-1-(trifluoromethyl)ethylidene]benzenamine ($(CF_3)_2C{=}NC_6H_4X$, **1-X**) was accelerated by both electron-donating (ED) and electron-withdrawing (EW) substituents on the aniline ring.[10] The Hammett plot in Fig. 1 showed a V-shaped behavior, which clearly indicated a change of the mechanism with the substituents. Asano and

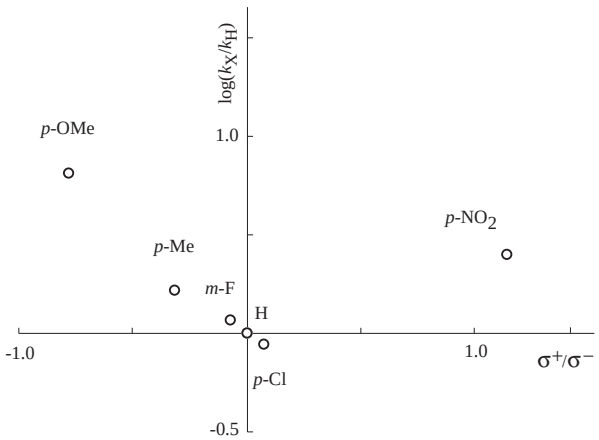

Fig. 1. Hammett plot for thermal isomerization of **1-X** in pyridine at 25 °C. For electron-donating and electron-withdrawing substituents, σ^+ and σ^- were used, respectively.

his co-workers more recently measured the rates of a large number of substituted *N*-[(4-nitrophenyl)methylene]benzenamine (p-$NO_2C_6H_4CH{=}NC_6H_4X$, **2-X**), and showed that here again the points for substrates with a strongly ED or EW substituent on the aniline ring deviated upwards from the correlation line (Fig. 2).[9]

A question of how a reaction mechanism changes with a subtle change in the substrate structure, e.g., by substituents, has been one of the central issues in physical organic chemistry. In general, there are two possible interpretations for the mechanism switching. First, the reaction proceeds via two independent pathways, and the relative importance of the two pathways changes with the substituents. In an alternative inter-

Published on the web October 4, 2005; DOI 10.1246/bcsj.78.1851

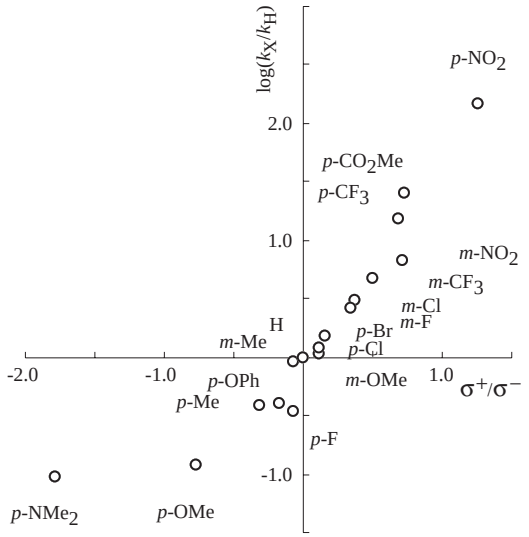

Fig. 2. Hammett plot for thermal isomerization of **2-X** in benzene at 25 °C. For electron-donating and electron-withdrawing substituents, σ^+ and σ^- were used, respectively.

pretation, there is a single reaction pathway for the reaction, and the nature of the TS changes smoothly with the substituents. Such a mechanistic issue has been raised in a borderline S_N1–S_N2 mechanism, in which an isopropyl or a benzyl substrate shows a borderline character.[11] These borderline substrates react through either concurrent S_N1 and S_N2 pathways or through a TS with intermediate character. The distinction of the two possible interpretations by experiment is intrinsically difficult, since what we obtain from experiment is the statistical average of a large number of events. Computational methods are more suitable for such an investigation, because they give us detailed information on the TS structures and the reaction pathways. However, the computational analysis of the borderline nucleophilic substitution reactions is complex, because the comparison of the calculated reactivities of unimolecular and bimolecular reactions is not straightforward, and also because a large solvent effect involved in the reactions prevents reliable computations. In contrast, the thermal C=N isomerizations are computationally accessible and serve as a good example of borderline reactions, since they are unimolecular reactions carried out in nonpolar aprotic solvents. In the present study, we carried out DFT calculations on the C=N isomerization reactions of $(CF_3)_2C{=}NC_6H_4X$ (**1-X**), *p*-$NO_2C_6H_4CH{=}NC_6H_4X$ (**2-X**), and $YC_6H_4CCF_3{=}NC_6H_4X$ (**3-X**), and analyzed how the mechanism changes with the substituents.

Computational Method

Substituted reactants and TSs for the three reaction systems were fully optimized at the HF and the B3LYP nonlocal hybrid density functional theory[12] with the 6-31G* basis set[13] using the Gaussian 98 suite of programs.[14] For *N*-[2,2,2-trifluoro-1-(trifluoromethyl)ethylidene]benzenamine (**1**, X = H), the reactant and the TS were fully optimized at various methods (HF/6-31G*, HF/6-31+G*, B3LYP/6-31G*, B3LYP/6-31+G*, B3LYP/6-311+G**, MP2/6-31G*, and MP2/6-31+G*) to see the effects of the theory and the basis sets. Full frequency analyses were carried out in all cases to confirm that the optimized structures were minima or saddle points. Thermochemical quantities, such as entropy, enthalpy, and free energy, were calculated from harmonic frequencies at respective levels.

Results and Discussion

Computations at different levels gave basically the same structures for **1** (X = H) and similar isomerization TS structures with a linear C=N–Ph and slightly twisted N–Ph conformation. The selected geometrical parameters and activation barriers are listed in Table 1. The activation barrier slightly depends on the computational level. Although B3LYP calculations tend to give lower barriers, the calculated barriers are qualitatively similar in magnitude to the experimental $\Delta H^{\ddagger}$ (58.6 ± 0.8 kJ mol^{-1}) and $\Delta G^{\ddagger}$ (64.4 ± 0.1 kJ mol^{-1}) in pyridine at 25 °C,[10] suggesting that the solvent effect is small in the reaction.

In Figs. 3 and 4 are illustrated plots of calculated relative reactivities ($-0.4343\delta\Delta H/RT$) against the experimental relative reactivities ($\log k_X/k_H$) for **1** and **2**. We use enthalpy rather than free energy in the substituent-effect analyses because the size of the entropy, and hence the free energy, depend much on low frequencies, which are less reliable than higher frequencies, especially for compounds with weak interactions, such as TS. The correlations gave reasonably good straight lines, indicating that the substituent effects are well reproduced by the present calculations. Furthermore, the slopes of the correlations are close to unity in both cases. The results suggest that the solvent effect is not important for the substituent effects of these reactions.

Table 1. Selected Geometrical Parameters and Activation Barriers for **1** (X = H) at Different Computational Methods[a)]

Computational method	Reactant		TS		Barrier height	
	θ	ϕ	θ	ϕ	$\Delta H^{\ddagger}$	$\Delta G^{\ddagger}$
HF/6-31G*	127.4	58.7	180.0	4.7	57.8	60.7
HF/6-31+G*	127.2	62.9	180.0	3.0	57.3	57.7
B3LYP/6-31G*	128.3	46.0	180.0	15.5	54.9	51.5
B3LYP/6-31+G*	129.0	47.4	180.0	15.5	48.1	45.2
B3LYP/6-311+G**	128.6	49.7	180.0	19.2	51.4	44.8
MP2/6-31G*	123.6	57.3	180.0	18.9	74.8	72.8
MP2/6-31+G*	122.9	62.0	180.0	28.6	73.2	69.5

a) Angles are in degree and energies are in kJ mol^{-1} at 25 °C.

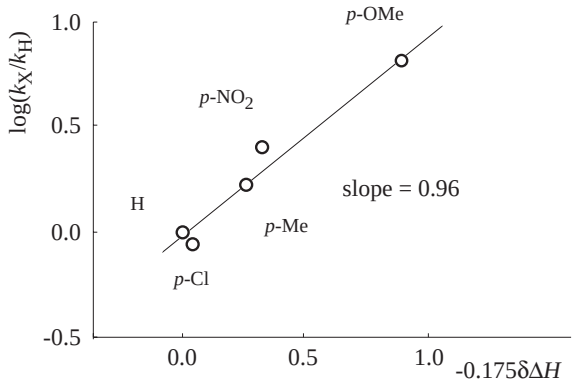

Fig. 3. Comparison of calculated relative activation enthalpy (B3LYP/6-31G*) and experimental relative reactivity for the C=N isomerization of **1** at 25 °C.

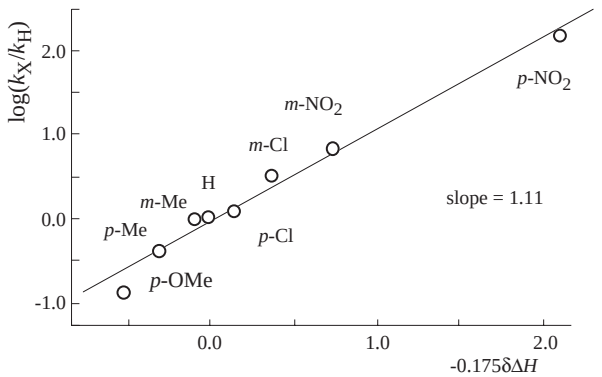

Fig. 4. Comparison of calculated relative activation enthalpy (B3LYP/6-31G*) and experimental relative reactivity for the C=N isomerization of **2** at 25 °C.

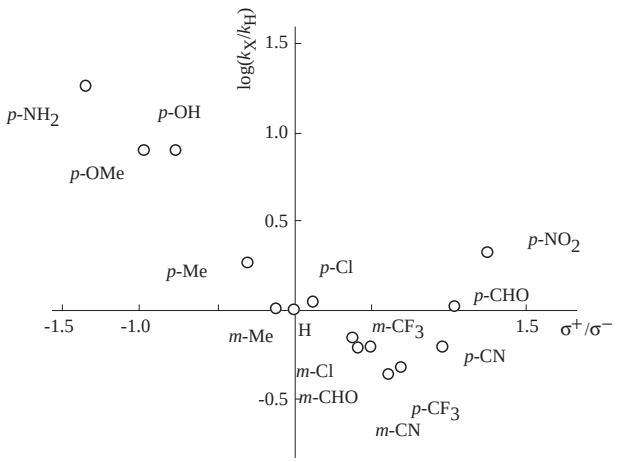

Fig. 5. Calculated Hammett plots for the C=N isomerization of **1-X** at 25 °C at B3LYP/6-31G*.

The Hammett plots for the C=N isomerization of $(CF_3)_2C{=}NC_6H_4X$ (**1-X**) at 25 °C obtained by the calculations are shown in Fig. 5. Here, we used σ^+ for ED substituents and σ^- for EW substituents, since the resonance interaction may be important for both cases, as discussed below, although the use of the standard Hammett σ values does not change the conclusions. With a large number of substituents than in the

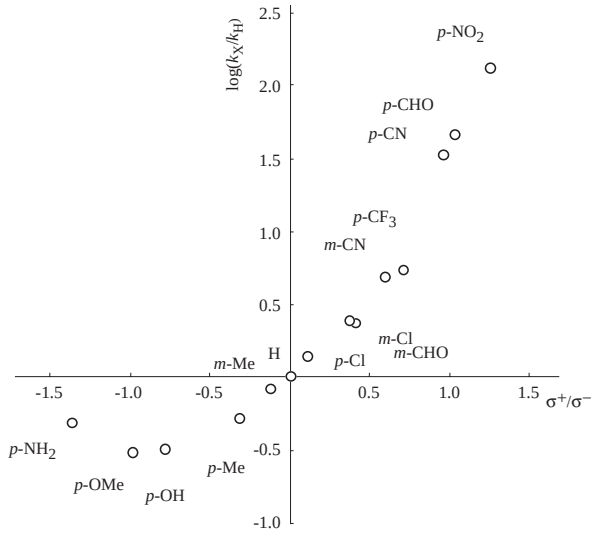

Fig. 6. Calculated Hammett plots for the C=N isomerization of **2-X** at 25 °C at B3LYP/6-31G*.

experiment, the calculated Hammett plots gave a clear V-shaped behavior, and thus nicely demonstrated that the reaction mechanism changes with the substituents. Figure 6 shows the Hammett-type plots for p-$NO_2C_6H_4C{=}NC_6H_4X$ (**2-X**) at 25 °C obtained by the calculations. Here again, the calculated results nicely reproduced the experimental substituent effects.

Although there are no corresponding experimental data available, the reactions of $YC_6H_4CCF_3{=}NC_6H_4X$ (**3**, Y = p-NO_2, H, or p-NH_2) were also examined computationally to see the effect of the structure of the benzylic moiety on the mechanistic change. The Hammett plots for **3** illustrated in Fig. 7 show clear V-shape behaviors for the three Y-substituted series. An examination of the three reactions reveals that the introduction of a more EW group at the benzylidene ring shifts the point of the mechanistic change to a less ED side of the substituent on the aniline ring, from X = p-OH with Y = p-NH_2 to X = H with Y = p-NO_2. In other words, with a more EW substituent (Y) on the carbon center, an ED substituent (X) on the aniline ring results in greater rate acceleration. The same trend can be seen when the plots of **2** (Y = p-NO_2) are compared with those of **3** (Y = p-NO_2); the introduction of CF_3 at the carbon center of C=N shifts the point of the mechanistic change from p-OH (**2**, Y = p-NO_2) to H (**3**, Y = p-NO_2).

In order to answer the question of how the mechanism changes with the substituents, we analyzed the TS structures and their variation with substituent X. In Scheme 1 are illustrated the structures of the reactant and the TS of three substituted *N*-[2,2,2-trifluoro-1-(trifluoromethyl)ethylidene]benzenamine. The reactant structures are similar, but the structures of the TSs differ qualitatively with X. For **1** (X = p-OH), the phenyl ring and the C=N double bond plane appear to lie in a parallel fashion to each other and to share a common plane in the TS, whereas for the p-NO_2 TS they are perpendicular. The TS of the p-CN derivative takes a conformation intermediate between the two extremes. Thus, the torsional angle (ϕ) at the TS varies with the substituent. In Fig. 8 are illustrated the energy variations with the torsional angle ϕ in the linear conformation ($\theta = 180°$) of $(CF_3)_2C{=}NC_6H_4X$; the angle ϕ

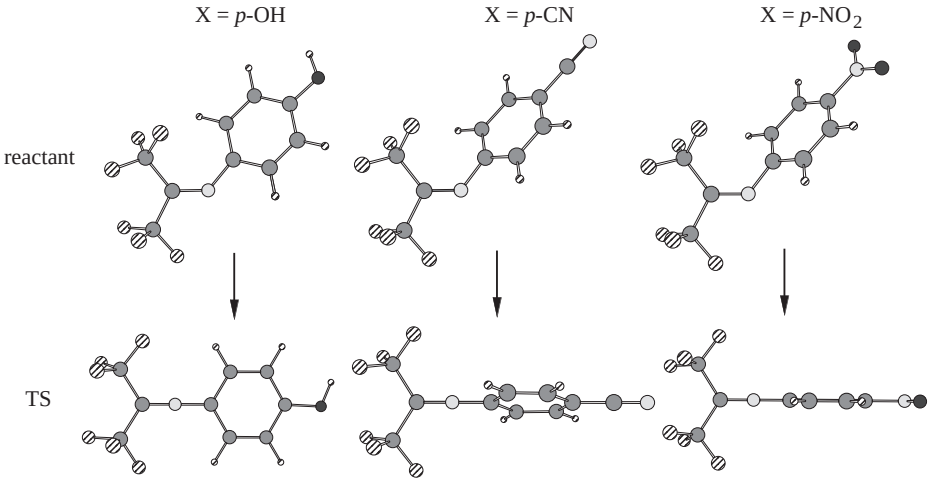

Scheme 1. Structures of reactant and TS for substituted **1**.

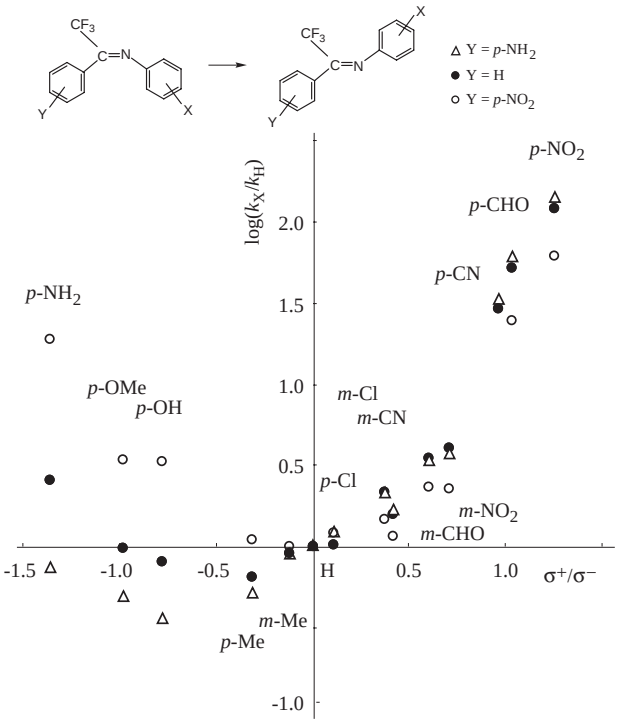

Fig. 7. Calculated Hammett plots for the C=N isomerization of **3** at 25 °C: triangle, Y = *p*-NH_2; filled circle, Y = H; open circle, Y = *p*-NO_2 at B3LYP/6-31G*.

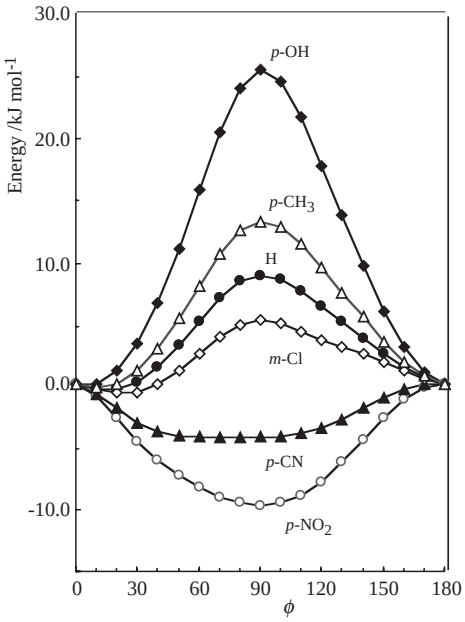

Fig. 8. Electronic energy variation with the torsional angle ϕ in the linear conformation ($\theta = 180°$) of **1** calculated at B3LYP/6-31G*.

with minimum energy corresponds to the torsional angle at the TS for each derivative. The energy of the *p*-OH derivative varies through a sharp minimum near at $\phi = 0°$, whereas the *p*-NO_2 derivative has a minimum at $\phi = 90°$, corresponding to the parallel TS and perpendicular TS structures for these substituted derivatives. The *p*-CN derivative, on the other hand, has a broader and shallow minimum at $\phi = 73.7°$. Thus, the TS structure of the borderline substrate is flexible, and may show a wide range of intermediate character between the two mechanistic extremes. The parallel structure is preferred for the *p*-OH derivative because it allows the maximum conjugation between the *p*-OH substituted aniline ring and the $(CF_3)_2C{=}N$ moiety, whereas the *p*-NO_2 derivative takes a perpendicular conformation, which allows conjugation between the lone-pair electrons of the sp-hybridized N and *p*-NO_2 aniline ring. In Table 2 are listed the activation energies and the angle ϕ for $(CF_3)_2C{=}NC_6H_4X$. The results in Fig. 8 and Table 2 clearly indicate that the TS structure changes smoothly with a change in substituent X. It should be noted that no substituted derivative has two minima in the energy plots in Fig. 8, which confirms that the mechanistic change detected by the V-shaped Hammett plots occurs through a variation of the single TS structure, and is not due to the competition of two reaction pathways. In a similar manner, the torsional angle ϕ at the TSs for **2** and **3** increases as X becomes more EW: $\phi = 29.4°$ for **2**, X = *p*-NH_2 and 89.8° for **2**, X = *p*-NO_2; $\phi = 20.3°$ for **3**, Y = *p*-NH_2, X = *p*-NH_2 and 89.6° for **3**, Y = *p*-NH_2, X = *p*-NO_2; $\phi = 13.0°$ for **3**, Y = H, X = *p*-NH_2 and 89.6°

Table 2. Torsional Angles ϕ at the TS and Activation Enthalpies and Free Energies of Activation for the Isomerization of **1-X**[a)]

X	ϕ	$\Delta H^{\ddagger}$	$\Delta G^{\ddagger}$
p-NH_2	3.6	47.7	46.8
p-OH	4.5	49.8	48.7
p-OMe	4.6	49.8	48.6
p-Me	9.2	53.6	48.8
m-Me	14.0	54.9	51.5
H	15.5	54.9	51.5
p-Cl	14.7	54.7	51.4
m-CHO	19.4	56.1	52.6
m-Cl	23.5	55.8	53.0
m-CF_3	27.9	56.1	54.4
m-CN	31.5	57.0	55.5
p-CF_3	37.9	56.8	51.9
p-CN	73.7	53.4	49.3
p-CHO	88.9	54.8	50.7
p-NO_2	90.0	53.1	51.1

a) Torsional angles in degree and energies in kJ mol^{-1}.

for **3**, Y = H, X = *p*-NO_2; and $\phi = 8.7^{\circ}$ for **3**, Y = H, X = *p*-NH_2 and 89.6° for **3**, Y = H, X = *p*-NO_2.

The change from the perpendicular to the planar mechanism in the inversion scheme is consistent with a previous mechanistic assignment by Asano et al.,[6,9] who interpreted the nonlinear behaviors in the Hammett plots for **1** and **2** as arising from TS structural variations. The present study confirms the interpretation based on thorough calculations of the substituent effects, and reveals that the mechanistic change arises from the change of the character of a single TS, not from the change in a relative importance of two competitive reaction pathways.

The study was supported by a Grant-in-Aid for Scientific Research from the Ministry of Education, Culture, Sports, Science and Technology, Japan, and by Rikkyo University Frontier Project "Life's Adaptation Strategies to Environmental Changes." The calculations were carried out in part at the Research Center for Computational Science, Okazaki National Research Institute.

References

1 W. G. Herkstroeter, *J. Am. Chem. Soc.*, **95**, 8686 (1973).
2 A. V. Prosyanik, S. V. Loban', D. V. Fedoseenko, and V. I. Markov, *Zh. Org. Khim.*, **21**, 709 (1985).
3 A. V. Prosyanik and S. V. Loban', *Zh. Org. Khim.*, **21**, 1045 (1985).
4 A. V. Prosyanik, N. Yu. Kol'tsov, and V. A. Romanchenko, *Zh. Org. Khim.*, **22**, 1474 (1986).
5 T. Asano, T. Okada, and W. G. Herkstroeter, *J. Org. Chem.*, **54**, 379 (1989).
6 T. W. Saddle, H. Doine, S. D. Kinrade, A. Sera, T. Asano, and T. Osaka, *J. Am. Chem. Soc.*, **112**, 2378 (1990).
7 H.-J. Hoffmann, T. Asano, and R. Cimiraglia, *J. Chem. Soc., Chem. Commun.*, **1991**, 295.
8 H.-J. Hoffmann, T. Asano, R. Cimiraglia, and R. Bonaccorsi, *Bull. Chem. Soc. Jpn.*, **66**, 130 (1993).
9 T. Asano, H. Furuta, H.-J. Hoffmann, R. Cimiraglia, Y. Tsuno, and M. Fujio, *J. Org. Chem.*, **58**, 4418 (1993).
10 G. E. Hall, W. J. Middleton, and J. D. Roberts, *J. Am. Chem. Soc.*, **93**, 4778 (1971).
11 See: for example, J. March, "Advanced Organic Chemistry," 3rd ed, Wiley, New York (1985), Chap. 10.
12 A. D. Becke, *J. Chem. Phys.*, **98**, 5648 (1993); A. D. Becke, *Phys. Rev. A*, **38**, 3098 (1993); C. Lee, W. Yang, and R. G. Parr, *Phys. Rev. B*, **37**, 785 (1988).
13 M. M. Francl, W. J. Pietro, W. J. Hehre, J. S. Binkley, M. S. Gordon, D. J. Defrees, and J. A. Pople, *J. Chem. Phys.*, **77**, 3654 (1982).
14 M. J. Frisch, G. W. Trucks, H. B. Schlegel, G. E. Scuseria, M. A. Robb, J. R. Cheeseman, V. G. Zakrzewski, J. A. Montgomery, Jr., R. E. Stratmann, J. C. Burant, S. Dapprich, J. M. Millam, A. D. Daniels, K. N. Kudin, M. C. Strain, O. Farkas, V. Tomasi, M. Barone, R. Cossi, B. Cammi, C. Mennucci, C. Pomelli, S. Adamo, J. Clifford, J. Ochterski, G. A. Petersson, P. Y. Ayala, Q. Cui, K. Morokuma, D. K. Malick, A. D. Rabuck, K. Raghavachari, J. B. Foresman, J. Cioslowski, J. V. Ortiz, B. B. Stefanov, G. Liu, A. Liashenko, P. Piskorz, I. Komaromi, R. Gomperts, R. L. Martin, D. J. Fox, T. Keith, M. A. Al-Laham, C. Y. Peng, A. Nanayakkara, C. Gonzalez, M. Challacombe, P. M. W. Gill, B. Johnson, W. Chen, M. W. Wong, J. L. Andres, C. Gonzalez, M. Head-Gordon, E. S. Replogle, and J. A. Pople, "Gaussian 98, Revision A.6," Gaussian, Inc., Pittsburgh PA (1998).